**NAVAL AIR WARFARE CENTER AIRCRAFT DIVISION
PATUXENT RIVER, MARYLAND**

TECHNICAL REPORT

REPORT NO: NAWCADPAX/TR-2013/252

COATED 4340 STEEL

by

**E. U. Lee
C. Lei
M. Stanley
B. Pregger
C. Matzdorf**

26 August 2013

DEPARTMENT OF THE NAVY
NAVAL AIR WARFARE CENTER AIRCRAFT DIVISION
PATUXENT RIVER, MARYLAND

NAWCADPAX/TR-2013/252
26 August 2013

COATED 4340 STEEL

by

E. U. Lee
C. Lei
M. Stanley
B. Pregger
C. Matzdorf

RELEASED BY:

_____ 26 Aug 2013
KEVIN J. KOVALESKI / AIR-4.3.4 / DATE
Head, Materials Engineering Division
Naval Air Warfare Center Aircraft Division

REPORT DOCUMENTATION PAGE		Form Approved OMB No. 0704-0188

Public reporting burden for this collection of information is estimated to average 1 hour per response, including the time for reviewing instructions, searching existing data sources, gathering and maintaining the data needed, and completing and reviewing this collection of information. Send comments regarding this burden estimate or any other aspect of this collection of information, including suggestions for reducing this burden, to Department of Defense, Washington Headquarters Services, Directorate for Information Operations and Reports (0704-0188), 1215 Jefferson Davis Highway, Suite 1204, Arlington, VA 22202-4302. Respondents should be aware that notwithstanding any other provision of law, no person shall be subject to any penalty for failing to comply with a collection of information if it does not display a currently valid OMB control number. **PLEASE DO NOT RETURN YOUR FORM TO THE ABOVE ADDRESS.**

1. REPORT DATE 26 August 2013	2. REPORT TYPE Technical Report	3. DATES COVERED
4. TITLE AND SUBTITLE Coated 4340 Steel		5a. CONTRACT NUMBER
		5b. GRANT NUMBER
		5c. PROGRAM ELEMENT NUMBER
6. AUTHOR(S) E. U. Lee C. Lei M. Stanley B. Pregger C. Matzdorf		5d. PROJECT NUMBER
		5e. TASK NUMBER
		5f. WORK UNIT NUMBER
7. PERFORMING ORGANIZATION NAME(S) AND ADDRESS(ES) Naval Air Warfare Center Aircraft Division 48066 Shaw Road, Unit 5 Patuxent River, Maryland 20670-19081		8. PERFORMING ORGANIZATION REPORT NUMBER NAWCADPAX/TR-2013/252
9. SPONSORING/MONITORING AGENCY NAME(S) AND ADDRESS(ES) Naval Air Systems Command 47123 Buse Road Unit IPT Patuxent River, Maryland 20670-1547		10. SPONSOR/MONITOR'S ACRONYM(S)
		11. SPONSOR/MONITOR'S REPORT NUMBER(S)

12. DISTRIBUTION/AVAILABILITY STATEMENT

Approved for public release; distribution is unlimited.

13. SUPPLEMENTARY NOTES

14. ABSTRACT

A study was conducted to evaluate the effects of three coating systems on the mechanical property, fatigue, and stress corrosion cracking (SCC) of 4340 steel. These coating systems were electroplated cadmium and chromate passivation, cadmium with chromate primer, and cadmium, chromate primer and polyurethane topcoat. The three coating systems reduced the bending strength and hardness of the base metal, 4340 steel, in air. Their respective effects on the fatigue resistance of bare 4340 steel were similar in both of the employed environments, air and 3.5% NaCl solution. In addition, they were found to reduce the fatigue resistance of bare 4340 steel in air, but protect the substrate partly from aggressive environmental attack in 3.5% NaCl solution. The reduction of bending strength, hardness and fatigue resistance in air is attributed to hydrogen embrittlement, induced by Cd-electroplating. The SCC resistance was found to be enhanced more by each additional coating on the initial electroplated cadmium.

15. SUBJECT TERMS

4340 Steel; Mechanical Property; Fatigue; Stress Corrosion Cracking (SCC)

16. SECURITY CLASSIFICATION OF:			17. LIMITATION OF ABSTRACT	18. NUMBER OF PAGES	19a. NAME OF RESPONSIBLE PERSON Eun Lee
a. REPORT	b. ABSTRACT	c. THIS PAGE			19b. TELEPHONE NUMBER (include area code)
Unclassified	Unclassified	Unclassified	SAR	36	(301) 342-8069

Standard Form 298 (Rev. 8-98)
Prescribed by ANSI Std. Z39-18

SUMMARY

Bare 4340 steel specimens were initially coated with electroplated cadmium and passivated in a chromate solution. Additional specimens were then coated with chromate primer or chromate primer and polyurethane topcoat. The respective roles of coatings were studied by means of bending, hardness, fatigue and Stress Corrosion Cracking (SCC) tests and examining the post-test fractographs. Compared to the bare metal samples, coatings reduced the bending strength, hardness, and fatigue resistance in air, whereas they resisted corrosion fatigue in 3.5% NaCl solution. The reduction of bending strength, hardness and fatigue resistance in air is attributable to hydrogen embrittlement, induced by the electroplated cadmium. The better corrosion fatigue endurance in 3.5% NaCl solution is attributable to the protective action of the passivated cadmium and organic coatings against the aggressive environmental attack. On the one hand, the respective effects of the coatings on the fatigue resistance of bare 4340 steel were found to be similar in both of the employed environments, air and 3.5% NaCl solution. The SCC resistance was improved by each additional coating: lowest for the passivated cadmium, intermediate with the addition of the chromate primer, and greatest with the addition of the polyurethane topcoat.

Contents

ACKNOWLEDGEMENTS

INTRODUCTION

Many aircraft structural components are made from low alloy high strength steels with yield and ultimate tensile strength around 250 and 290 ksi, respectively (references 1 and 2). One of them is 4340 steel, which is a Ni-Cr-Mo low alloy steel that can be heat treated to reach tensile strength levels of approximately 280 ksi. However, the main drawback of high strength steels is their intrinsic susceptibility to environmentally assisted embrittlement or cracking, such as hydrogen embrittlement, Stress Corrosion Cracking (SCC), and corrosion fatigue.

Hydrogen embrittlement is a process in which atomic hydrogen generated on the steel surface by cathodic reactions diffuses into the microstructure and degrades its mechanical properties. Consequently, a sudden and unpredictable failure of the component can take place. Atomic hydrogen can be generated during electroplating processes or when the steel components are exposed to any aqueous fluid in service (references 3 and 4). Although hydrogen uptake by the steel represents a potential problem, baking the electroplated specimens enhances the removal of the absorbed hydrogen from the steel and consequently a recovery of its original mechanical properties takes place (references 3 and 5). However, the baking process is often complicated by slow diffusion of hydrogen through the electrodeposit which can trap the hydrogen, making its elimination difficult.

Pores or flaws in the sacrificial coating could directly expose the steel component to corrosive fluids, generating localized galvanic cells between the steel and the coating. As a result, hydrogen evolution and its partial absorption take place on the steel surface when simultaneous anodic dissolution of the coating proceeds. This phenomenon has been defined as hydrogen re-embrittlement and arises during operating conditions.

SCC is failure by cracking under the combined action of corrosion and an applied or a residual stress. It is normally associated with several mechanisms: anodic electrochemical dissolution of crack path, rupture of brittle corrosion product film exposing bare metal, and hydrogen embrittlement (references 3, 4, and 6). The latter mechanism of SCC is the most likely for high strength steels. The crack path may be either intergranular or transgranular, depending on the metal and the corrosive medium.

Corrosion fatigue is a phenomenon of cracking under the combined action of a cyclic stress and a corrosive environment. The resulting damage may be a simple superposition of fatigue cracking and corrosion attack or it may be a more complex synergistic interaction of these two modes. For high strength steels, corrosion fatigue crack growth in aqueous environments appears to be controlled by the rate of reactions of the environment with the newly created crack surfaces (reference 7).

To avoid the direct exposure to aggressive environments and protect the surfaces from environmentally assisted embrittlement or cracking, high strength steel components are usually protected with coatings. The coatings can be applied in a range of ways including organic coating by painting and spraying techniques (reference 8), metallic sputtering, plasma vapor

deposition (reference 9), chemical vapor deposition, hot dip galvanizing, anodizing, composite coatings (references 10 and 11), organic metal flake coatings (e.g., Dacromet) and electroplating with or without conversion coatings or passivations (reference 12).

Electroplating is commonly used, because it is generally fast, cheap, and effective in many applications. A wide variety of steel components are currently protected from corrosion using coatings of electroplated cadmium. Cadmium provides excellent corrosion protection and its sacrificial nature means that if the coating is damaged, cadmium will still protect the steel substrate by corroding preferentially. Cadmium also has excellent galvanic compatibility with aluminum alloys, which is especially useful in aerospace applications. All these advantages, together with the self-lubrication properties of cadmium which aids uniformly tightening threaded fasteners, make this metal the primary protective coating for aerospace applications (reference 5). Considering the advantage of using cadmium-plating, there would be value in determining whether the performance of the Cd-plated steel can be further improved by alternative sacrificial coatings as well as investigate the role of primers and topcoats in SCC and corrosion fatigue. This study was initiated to:

- Clarify the roles of electroplated cadmium and chromate passivation, chromated primer and polyurethane topcoat in the resistance of bare 4340 steel to environmentally assisted embrittlement or cracking.
- Establish an optimum coating system for 4340 steel, which can provide the best resistance to environmentally assisted embrittlement or cracking.

A follow-on effort is planned to investigate the effect of a non-chromate primer and zinc-nickel plating with non-chromate passivation as alternatives to the chromate primer and cadmium plating with chromate passivation.

EXPERIMENTAL PROCEDURE

MATERIAL AND SPECIMENS

As the base or substrate material of the specimens, a 4340 steel plate of 2" x 6" x 12" was purchased from Metalmen Sales, Inc., New York, NY. Its chemical composition is shown in Table 1, and its microstructure in Figure A-1.

Table 1: Chemical Composition of 4340 Steel

Element	Weight (%)
C	0.42
Mn	0.75
P	0.013
S	0.006
Si	0.22
Cu	0.17
Ni	1.67
Cr	0.83
Mo	0.21
Al	0.03
V	0.005
N	0.065
Cb	0.002
Sn	0.009
Fe	Balance

The plate was machined to round tension test specimens in longitudinal (L-) orientation, Figure A-2, round hourglass fatigue test specimens in L-orientation, Figure A-3, and square bar SCC test specimens in L-T orientation, Figure A-4. The specimens of each type were divided into four groups, one for the test of bare specimens and the other three for the tests of plated or coated specimens.

COATING

Three groups of specimens were subjected to the following three coating systems, respectively.

1. No. 1 coating system: electroplated cadmium, hydrogen embrittlement relief treatment and chromate passivation per Aerospace Material Specification AMS-QQ-P-416 (reference 13).

2. No. 2 coating system: No. 1 coating system and chromated epoxy primer per MIL-PRF-85582D Class C (reference 14).

3. No. 3 coating system: No. 2 coating system and gloss white polyurethane topcoat per MIL-PRF-85285E Type I (reference 15)
   [This is the standard protective coating system currently used on high strength steel Navy and Marine Corps aircraft components.]

MECHANICAL TEST

Single edge notched, square-bar (Charpy) specimens, bare or coated, were tested under four-point bending at ambient temperature in a RSL 1000 SI-Multi-Mode System, and the bending fracture strength was determined in air.

The Rockwell C-scale hardness of a bare specimen or a substrate of surface-treated specimen was measured at ambient temperature in a Rockwell Hardness Tester.

FATIGUE TEST

A closed-loop servo-hydraulic mechanical test machine, MTS, of 20 kip capacity, was employed for the fatigue test. The fatigue test was carried out with hourglass specimens under tension-tension cyclic loading at stress ratio 0.1 and frequency 10 Hz in air and aqueous 3.5% NaCl solution of pH 7.3. This test followed the ASTM E 466, Standard Practice for Conducting Force Controlled Constant Amplitude Axial Fatigue Tests of Metallic Materials (reference 16).

STRESS CORROSION CRACKING TEST

Since the cantilever bend or double cantilever beam SCC test takes a long time, an accelerated SCC test (reference 17) was conducted in a RSL 1000 SI-Multi-Mode Test System. This System included a bending frame, a tensile loading frame, and an electrolyte reservoir, a pump for electrolyte circulation, a saturated calomel electrode, a platinum counterelectrode, a PC, and a printer. The un-precracked, coated specimens were step-loaded until the load dropped in four-point bending under constant displacement control, while held at a given potential in aqueous 3.5% NaCl solution of pH 7.3. The load drop corresponded to the threshold stress intensity for SCC, K_{OSCC}, for the coated specimen. The K_{OSCC} and the net stress at failure, σ_{net}, were calculated, using the following equations:

$$K_{OSCC} = \sigma\sqrt{\pi a}*F(a/W)$$
$$\sigma_{net} = My/I_{net} = 6M/[B(W-a)^2]$$

where

σ: gross stress $= 6M/BW^2$
B: specimen thickness
W: specimen width
M: bending moment $= Px$
I_{net}: net moment of inertia
P: applied load
a: notch depth or crack length
x: moment arm length
$y = (W – a)/2$
$F(a/W) = 1.122 – 1.40(a/W) + 7.33(a/W)^2 – 12.08(a/W)^3 + 14.0(a/W)^4$

K_{OSCC} and σ_{net}, the threshold stress intensity for SCC at an un-precracked notch and the net stress at SCC failure, were taken as the measures of SCC resistance of the surface-treated specimen in this study.

FRACTOGRAPHY

The bending fracture, fatigue crack and SCC morphologies were examined with a JEOL JSM-6460LV scanning electron microscope, operated at an acceleration voltage of 20 kV.

EXPERIMENTAL RESULTS

MECHANICAL PROPERTIES

The measured bending strength and hardness are as follows:

	Coating System			
	Bare	No. 1	No. 2	No. 3
Bending Stress (ksi)	373	351	333	340
Hardness (Rc)	53	51	50	51

FATIGUE

The stress-life (S-N) curves are shown for the bare and coated (Nos. 1, 2, and 3) specimens, fatigue-tested in air and 3.5% NaCl solution, in Figures A-5, A-6, A-7 and A-8, respectively. These figures compare the fatigue strengths in air and 3.5% NaCl solution for the respective coating systems. In all cases, the fatigue strength is lower and the life is shorter in 3.5% NaCl solution.

In order to compare the fatigue strengths of bare and coated specimens in air and 3.5% NaCl solution, their stress-life curves are plotted together in Figures A-9 and A-10, respectively. These figures show that

- The fatigue strength is greater for the bare specimen in air, but it is greater for the coated specimens in 3.5% NaCl solution.
- The stress-life curves for the coated specimens nearly overlap each other in both of the test environments, air and 3.5% NaCl solution.

STRESS CORROSION CRACKING

The variation of threshold stress intensity for SCC, K_{OSCC}, and net stress, σ_{net}, with applied potential, V_{SCE}, is shown in Figures A-11(a) and (b), respectively. These figures show that:

- The SCC resistance is greatest with the full coating system, intermediate for electroplated cadmium with chromate primer, and lowest for electroplated cadmium throughout the applied potentials, ranging from -1.2 to -0.4 V.

FRACTOGRAPH

A typical SEM fractograph for the No. 2 coating system, followed by four-point bending fracture in air, shows mostly dimples of various sizes and scattered intergranular facets, some with secondary cracks along grain boundaries, Figure A-12.

Typical SEM fractographs for the No. 3 coating system, fatigue-tested in air and 3.5% NaCl solution, are shown in Figures A-13 and A-14, respectively. These figures indicate that:

- The fatigue crack was initiated at an inclusion at or near the surface of the base-metal in air and 3.5% NaCl solution, Figures A-13(a) and A-14(a).
- In the early stage of fatigue crack growth, scattered intergranluar cracking occurred near the fatigue crack initiation site in air and 3.5% NaCl solution. This is evidenced by intergranularly separated smooth grain facets and secondary cracks at the grain boundaries in scattered spots, Figures A-13(a) and A-14(a).
- Within the slow crack growth area, faint and poorly defined striations or striations-like features were formed in air, Figure A-13(b). On the other hand, intergranular cracking and formation of brittle striations occurred in 3.5% NaCl solution. This is evidenced by intergranularly separated grain facets, secondary cracks at grain boundaries and brittle striations on the fracture surface, Figure A-14(b).
- In the overload fracture area, microvoid coalescence occurred in air and 3.5% NaCl solution. This is evidenced by the dimples of various sizes, covering the entire fracture surface, Figures A-13(c) and A-14(c).

Typical fractographs for the No. 3 coating system, followed by RSL-SCC test at $V_{SCE} = -1.2$ V in 3.5% NaCl solution, are illustrated in Figure A-15. Figure A-15(a) shows the coating, partly separated from the substrate, several roughly parallel cracks, initiated from the substrate-surface and grown into the substrate, and a subsurface cracking zone of meridional plane-shape below the notch-tip. It is believed that 3.5% NaCl solution seeped through the parallel cracks into the subsurface cracking zone during the SCC test. The subsurface cracking zone is occupied by intergranular facets and secondary cracks along grain boundaries, Figure 15(b).

DISCUSSION

FATIGUE BEHAVIOR

EFFECTS OF COATINGS

The stress-life (S-N) curves for the three coating systems nearly overlap each other for the fatigue tests in each of the environments employed, air and 3.5% NaCl solution, Figures A-9 and A-10. From this observation, it is clear that the effects of the employed coatings on the fatigue strength and life of the bare specimen are similar in each of the environments employed.

The Nos. 1, 2, and 3 coating systems lower the fatigue strength and life in air compared to the bare specimen, Figure A-9. The SEM fractograph of No. 3 coating system specimen, fatigue-tested in air, shows scattered intergranularly separated smooth grain-facets and secondary cracks along grain boundaries, Figure A-13(a). Such a fractographic feature is typical of SCC (reference 18), hydrogen embrittlement (reference 19) and corrosion fatigue (reference 20). Since the fatigue test was conducted in air, the possibility of SCC and corrosion fatigue is very slim or none. Therefore, it is deducible that the reduction in fatigue strength and life is attributed to hydrogen embrittlement, induced during the process of the Cd-electroplating of the No. 3 coating system. The post-electroplating baking was said to have been done per LPS 430B (reference 21) and AMS-QQ-416 (reference 13). Accordingly, it is likely that the specifications are not quite adequate for the surface-treatment done or/and the post electroplating baking process was not carried out correctly. It remains to be clarified.

EFFECT OF ENVIRONMENT

The fatigue strength and life are reduced in 3.5% NaCl solution, compared to those in air, for the bare and coated specimens, Figures A-5, A-6, and A-8. This observation indicates that those specimens, bare and coated, are susceptible to corrosion fatigue in 3.5% NaCl solution. However, the susceptibility to corrosion fatigue is less for those coated specimens than for the bare specimen, Figure A-10, indicating the protective role of the coatings against corrosion fatigue.

MECHANICAL PROPERTIES

The bending strengths of the coated specimens are lower than that of bare specimens in air. In addition, the fractograph of No. 2 coating system specimen (Figure A-12), which was fractured under four-point bending in air, shows scattered intergranular facets. This reduction in bending strength is similar to that in the fatigue strength of the surface-treated specimen in air, Figure 9. Therefore, it is deducible that the reduction in bending strength and intergranular cracking are also attributed to the hydrogen embrittlement, induced during electroplating the cadmium, a part of the No. 2 coating system.

The hardness of the substrate of each coated specimen is lower than that of the bare specimen. This reduction in hardness is also similar to that in the fatigue strength of the surface-treated

specimen, Figure 9. Therefore, it is deducible that the reduction in hardness is also attributed to the hydrogen embrittlement, induced during electroplating the cadmium, a part of each coating system.

STRESS CORROSION CRACKING BEHAVIOR

It is observable that each additional coating or an additional layer of coating results in a greater SCC resistance, Figure A-11. Consequently, electroplated and passivated cadmium provides the least SCC resistance, an additional primer coating an intermediate resistance, and final additional polyurethane coating the greatest SCC resistance in 3.5% NaCl solution. This may be attributed to an additional isolation and protection by an additional layer of coating against the corrosive medium, 3.5% NaCl solution.

It is also significant to observe that:

- A cracking zone of meridional plane-shape was formed below the notch-tip of a square bar specimen, which was subjected to four-point bending at $V_{SCE} = -1.2$ V in a 3.5% NaCl solution, Figure 15(a).
- The cracking zone was occupied by intergranular facets, Figure 15(b).

This observation evidences the initiation and propagation of intergranular SCC in a subsurface zone of meridional plane-shape. Such a zone has been known to be formed by a Hertz line of constant maximum shear stress under a frictionless load from a rigid sphere (reference 22).

CONCLUSIONS

The effects of Nos. 1, 2, and 3 coating systems on the fatigue resistance of a bare 4340 steel specimen are similar in both of the employed environments, air and 3.5% NaCl solution. In other words, the chromate primer and polyurethane topcoat do not provide additional protection to the electroplated cadmium with a chromate passivation.

Electroplating of cadmium induces hydrogen embrittlement and reduces the bending strength, hardness and fatigue resistance of 4340 steel in air, cracking the base-metal intergranularly.

Bare and coated 4340 steels are susceptible to corrosion fatigue in 3.5% NaCl solution, though the coating protects the substrate and mitigates the susceptibility greatly. The mechanism of corrosion fatigue is intergranular cracking.

The SCC resistance of 4340 steel in 3.5% NaCl solution can be increased further by adding additional coatings, such as chromate epoxy primer and polyurethane topcoat, on the electroplated cadmium with chromate passivation. The SCC mechanism is intergranular cracking, initiated and propagated in a subsurface meridional plane-shape zone, under rising step four-point bending.

RECOMMENDATIONS

Check whether the post electroplating baking process, specified in the Aerospace Material Specification AMS-QQ-P-416 and the LPS 430B, Electrolytic and Electroless Plating Local Process Specification, is satisfactory for the Cd-electroplating on 4340 steel.

Assess the impact of substitute primer and sacrificial coating on corrosion fatigue and SCC, in particular leading alternative coatings qualified to MIL-PRE-23377 Class N and an electroplated zinc-nickel alloy passivated with a trivalent chromium solution which is being field tested at FRC-Southeast.

Additional basic research focused on the role of each layer in SCC resistance is also desired to improve the basic understanding of the mechanism of these coatings.

REFERENCES

1. D. Wiser: U. S. Air Force Flying Safety Magazine, 2004, Vol. 60, No. 68, pp. 7-11.

2. A. Wrigley: Aerospace Metals, American Metal Market, of May 1994.

3. L. L. Sherir: in Corrosion 1, Metal/Environment Reactions, Newnes-Butterworths, London, Second Edition, 1976, pp. 8:3-8:73.

4. H. Uhlig: in Corrosion Handbook, Second Edition, John Wiley & Sons, 2000, pp. 191-231.

5. L. L. Sherir: in Corrosion 2, Corrosion Control, Newnes-Butterworths, London, Second Edition, 1976, pp. 14:17-14:86.

6. B. F. Brown: in Stress-Corrosion Cracking in High Strength Steels and in Titanium and Aluminum Alloys, B. F. Brown, Ed., Naval Research Laboratory, Washington, D.C., 1972, pp. 1-16.

7. Robert P. Wei and Gunchoo Shim: in Corrosion Fatigue: Mechanics, Metallurgy, Electrochemistry and Engineering, ASTM STP 801, T. W. Crooker and B. N Leis, Eds., American Society for Testing and Materials, 1983, pp. 5-25.

8. B. Fitzsimons: PCE, Mar 1996, pp. 24-32.

9. Airco Technical, Physical Vapour Deposition, Airco Incorporated 1976.

10. A Sachian, M. Blidariun, E. Roman and C. Raducanu: Transactions of Institute of Metal Finishing, 1977, Vol. 75, No. 6, pp. 213-215.

11. C. T. Dervos, C. Kollia, S. Psarrou, P. Vassiliou and N. Spyrellis: Transactions of Institute of Metal Finishing, 1998, Vol. 76, No. 4, pp. 127-130.

12. M. Siluvai Michael, M. Pushpavanam and K. Balakrishnan: Bulletin of Electrochemistry, 1996, Vol. 12, No. 1-2, pp. 80-82.

13. Aerospace Material Specification, AMS-QQ-P-416, Plating, Cadmium (Electrodeposited), SAE International, Warrendale, PA, of Jul 2000.

14. Performance Specification, Primer Coatings: Epoxy, Waterborne, MIL-PRF-85582D, with Amendment 1, of 9 Jun 2006.

15. Performance Specification Coating: Polyurethane, Aircraft and Support Equipment, MIL-PRF-85285E, of 12 Jan 2012.

16. ASTM E466-96, "Standard Practice for Conducting Force Controlled Constant Amplitude Axial Fatigue Tests of Metallic Materials," 2003 Annual Book of ASTM Standards, Vol. 0301.

17. The Rising Step-Load Test, ASM Handbook, Vol. 8, Mechanical Testing, ASM International, of Jun 1995, pp. 539-40.

18. Metals Handbook, 8th Edition, Vol. 9, Fractography and Atlas of Fractographs, American Society for Metals, of Aug 1974, p. 91, 313-314, 323.

19. ASM Handbook, Vol. 12, Fractography, ASM International, of May 1992, p. 248.

20. Metals Handbook, 8th Edition, Vol. 9, Fractography and Atlas of Fractographs, American Society for Metals, of Aug 1974, p. 260.

21. LPS 430B, "Electrolytic and Electroless Plating Local Process Specification," Fleet Readiness Center South-East, Naval Air Station, Jacksonville, FL, of 1 Apr 2009.

22. ASM Handbook, Vol. 8, Mechanical Testing, ASM International, of Jun 1995, p. 72.

APPENDIX
FIGURES

THIS PAGE INTENTIONALLY LEFT BLANK
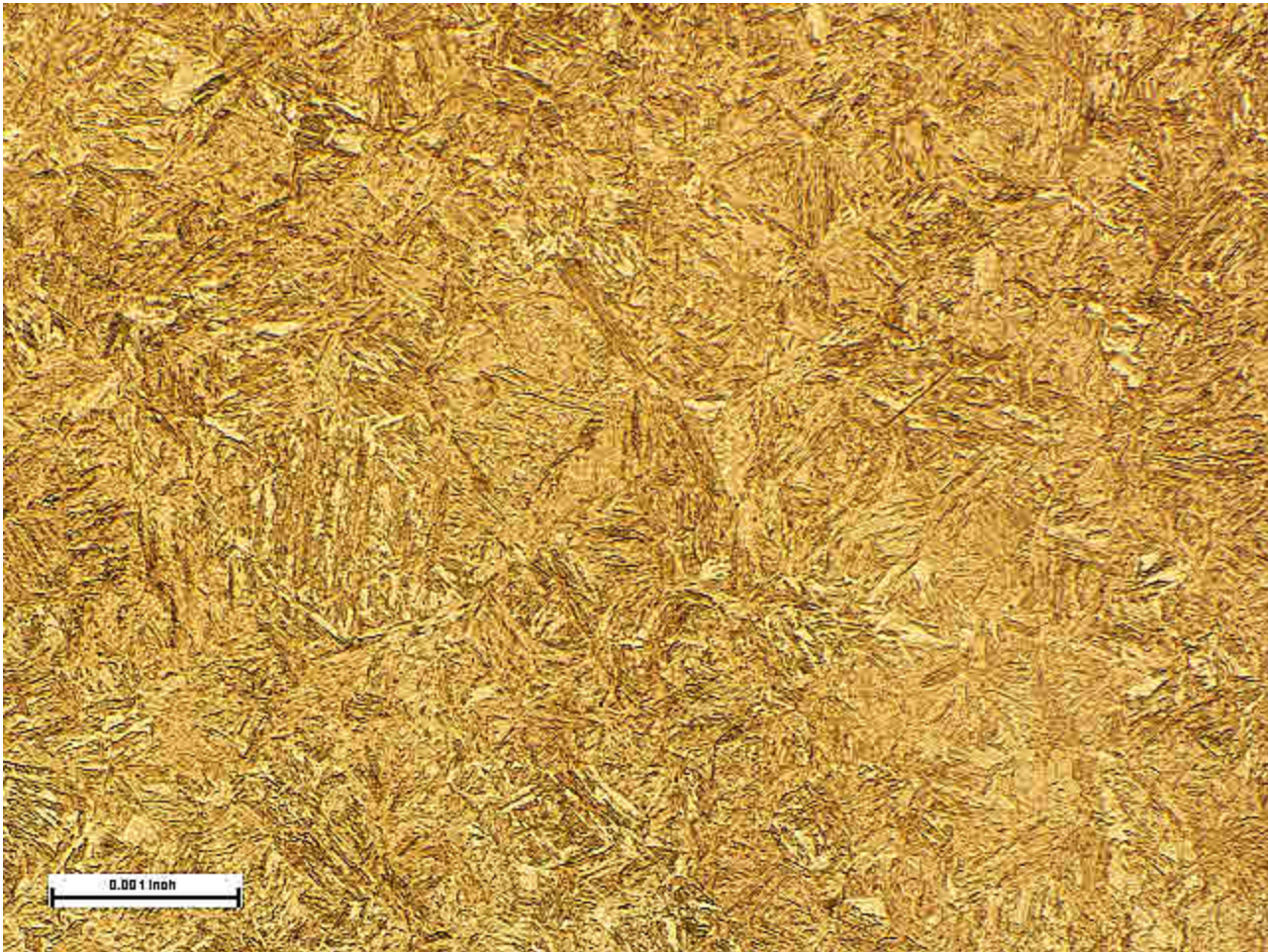
Figure 1: Microstructure of 4340 Steel

APPENDIX

$G = 1.000 \pm 0.005$"
$D = 0.250 \pm 0.005$"
$R = 3/16$"
$A = 1\ 1/4$"
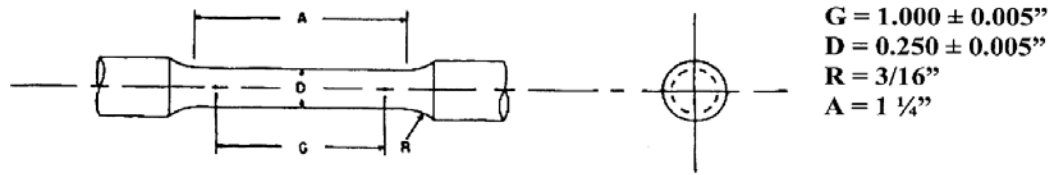
Figure 2. Round Tension Test Specimen

$L = 3\ 11/16$"
$D = 3/4$"
$R = 2.000 \pm 0.002$"
$B = 7/8$"
$d = 0.249 \sim 0.251$"
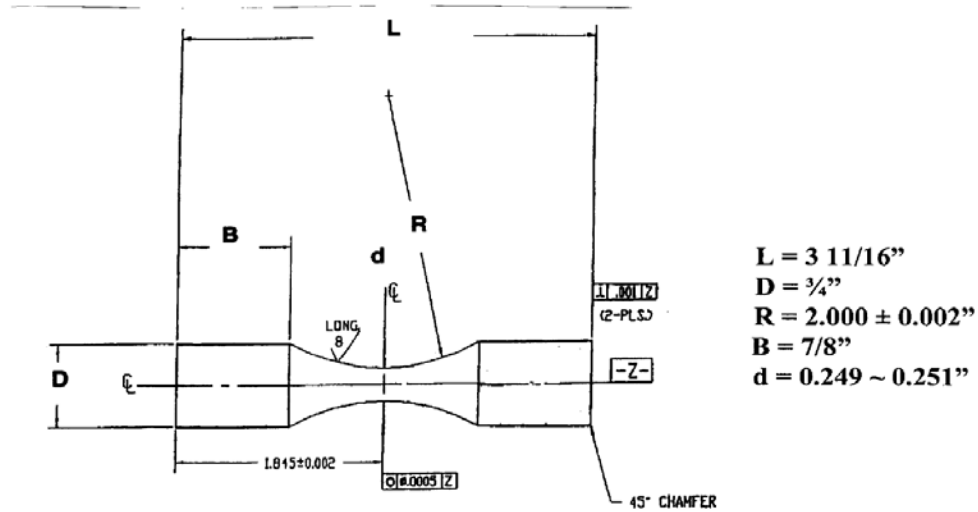
Figure 3. Round Hourglass Fatigue Test Specimen

APPENDIX

a = 0.209"
W = B = 0.398"
L = 2"
a/W = 0.525
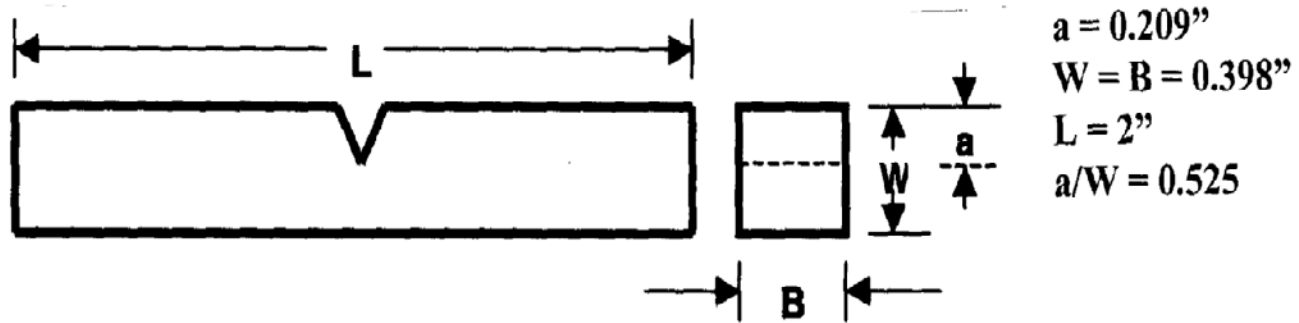
Figure 4. Square Bar Stress Corrosion Cracking Test Specimen
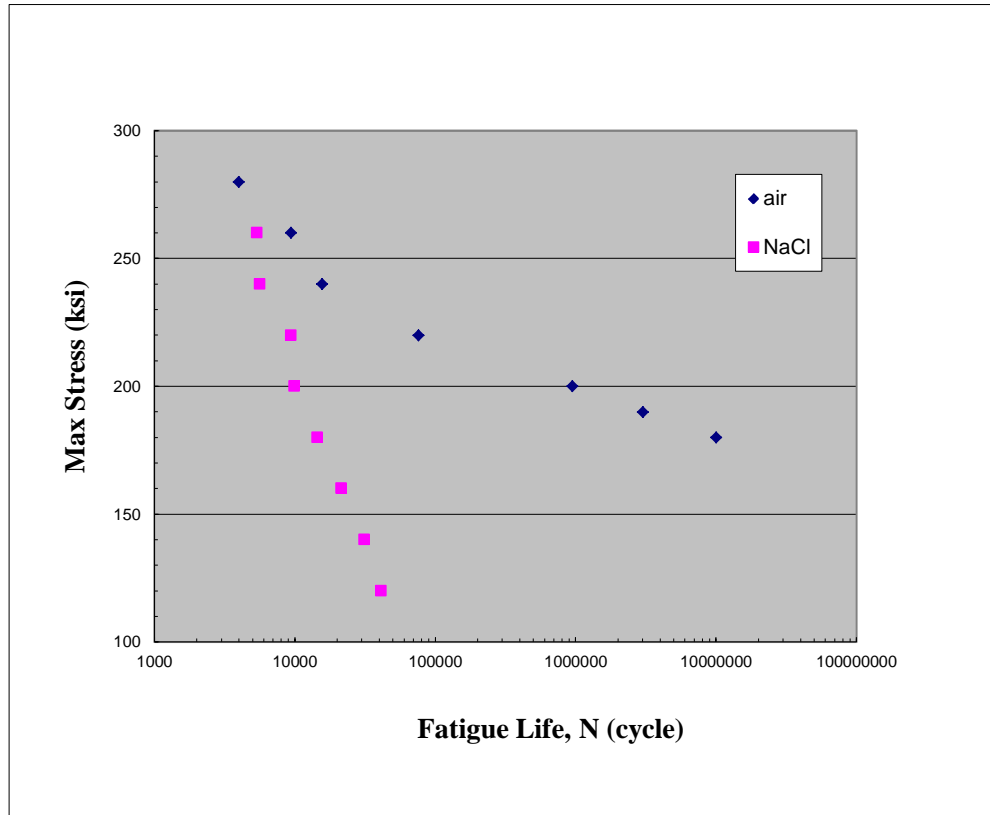
Figure 5: Stress-Life Fatigue Curves for Bare 4340 Steel
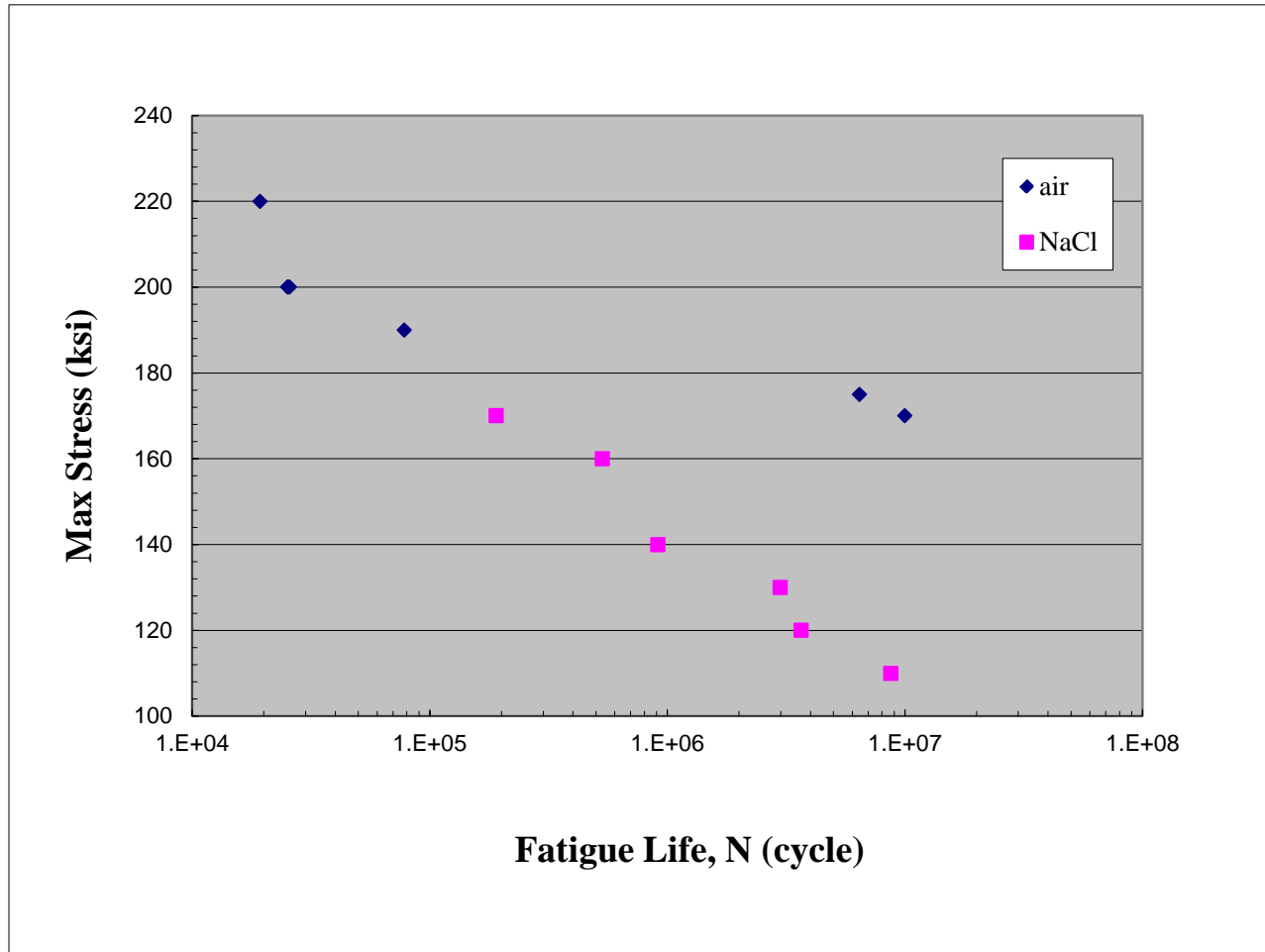
Figure 6: Stress-Life Fatigue Curves for No. 1 Surface-Treated 4340 Steel
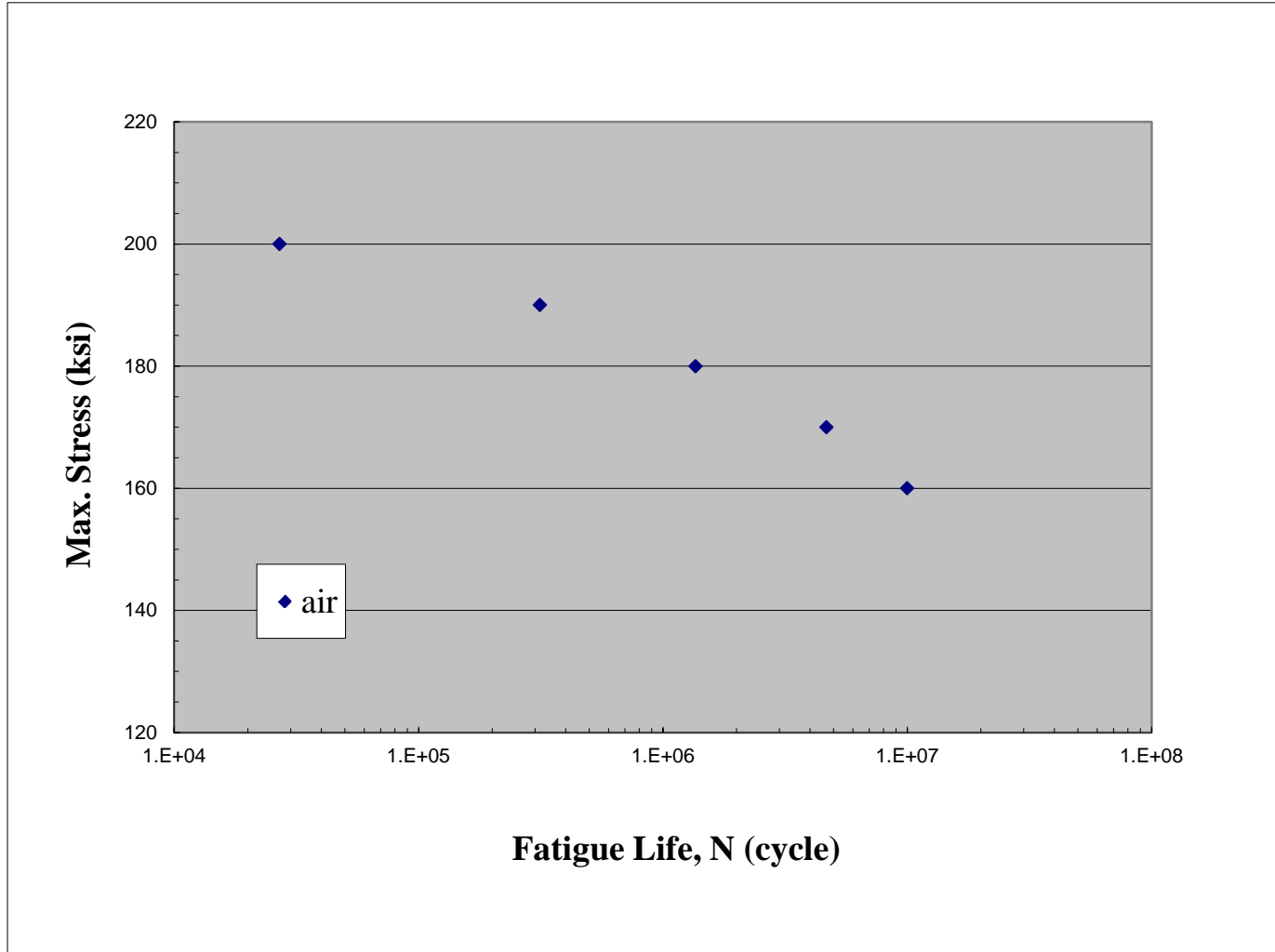
Figure 7: Stress-Life Fatigue Curve for No. 2 Surface-Treated 4340 Steel
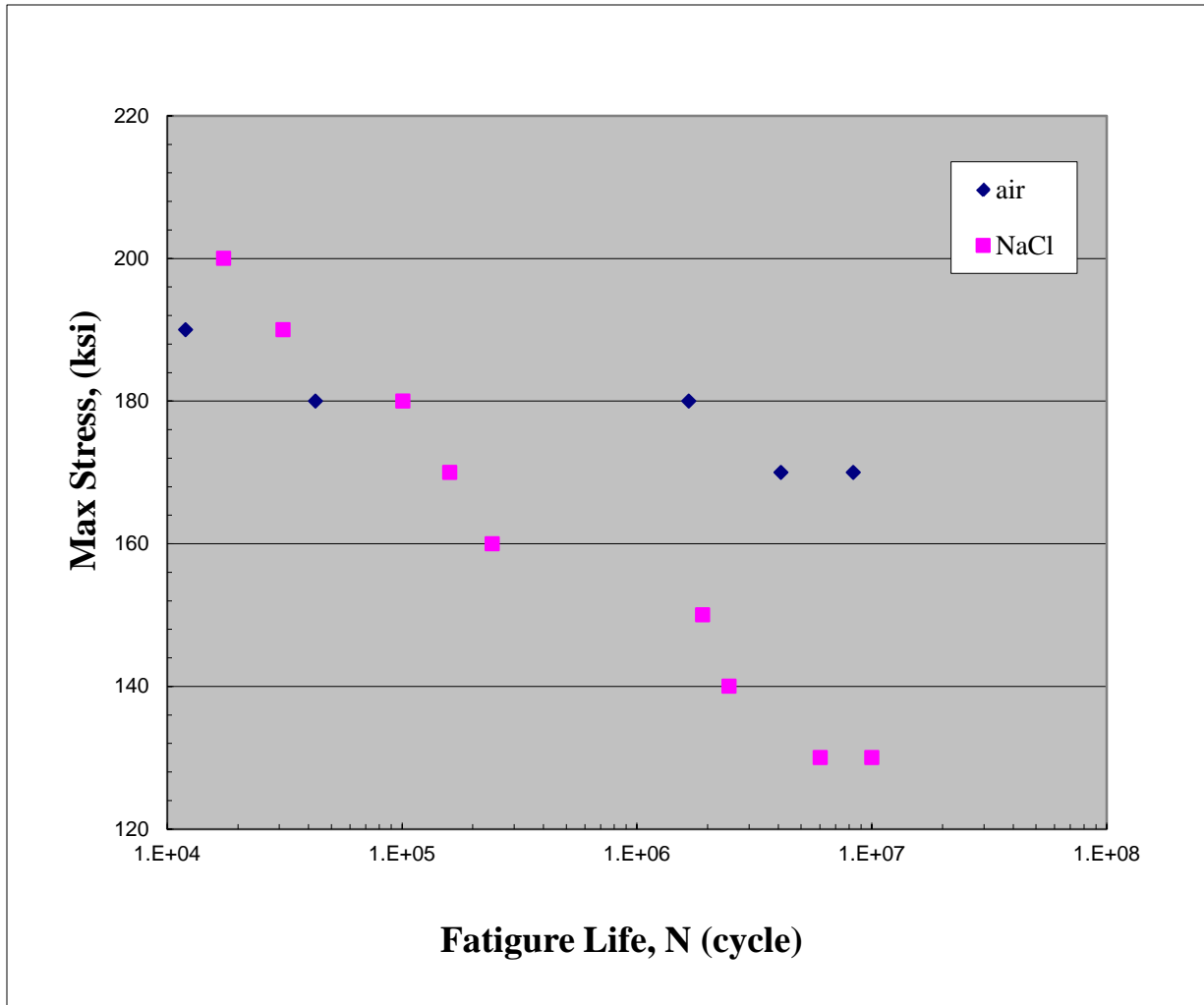
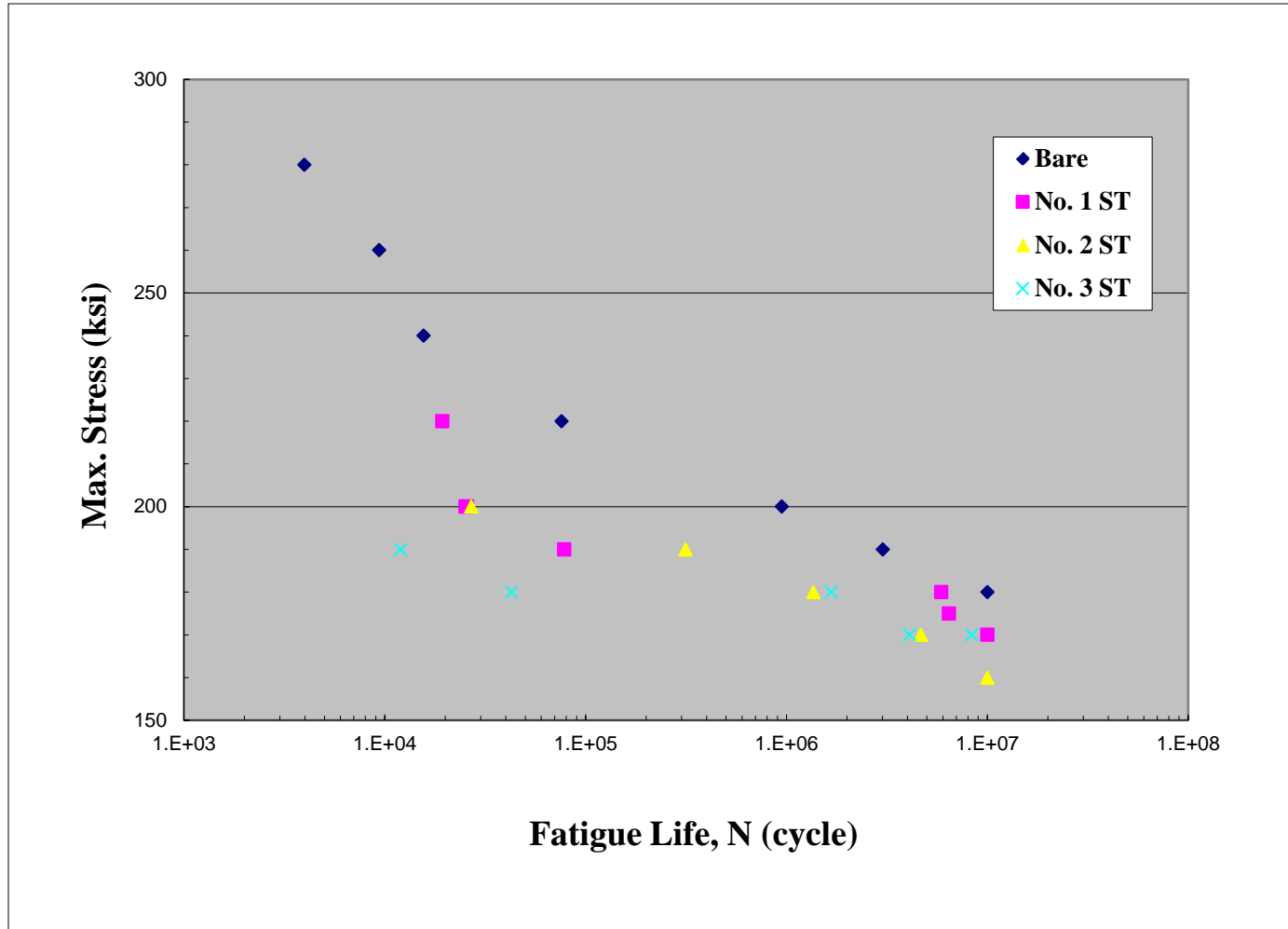Figure 8: Stress-Life Fatigue Curves for No. 3 Surface-Treated 4340 Steel

Figure 9: Stress-Life Fatigue Curves for Bare and Surface-Treated 4340 Steel Tested in Air
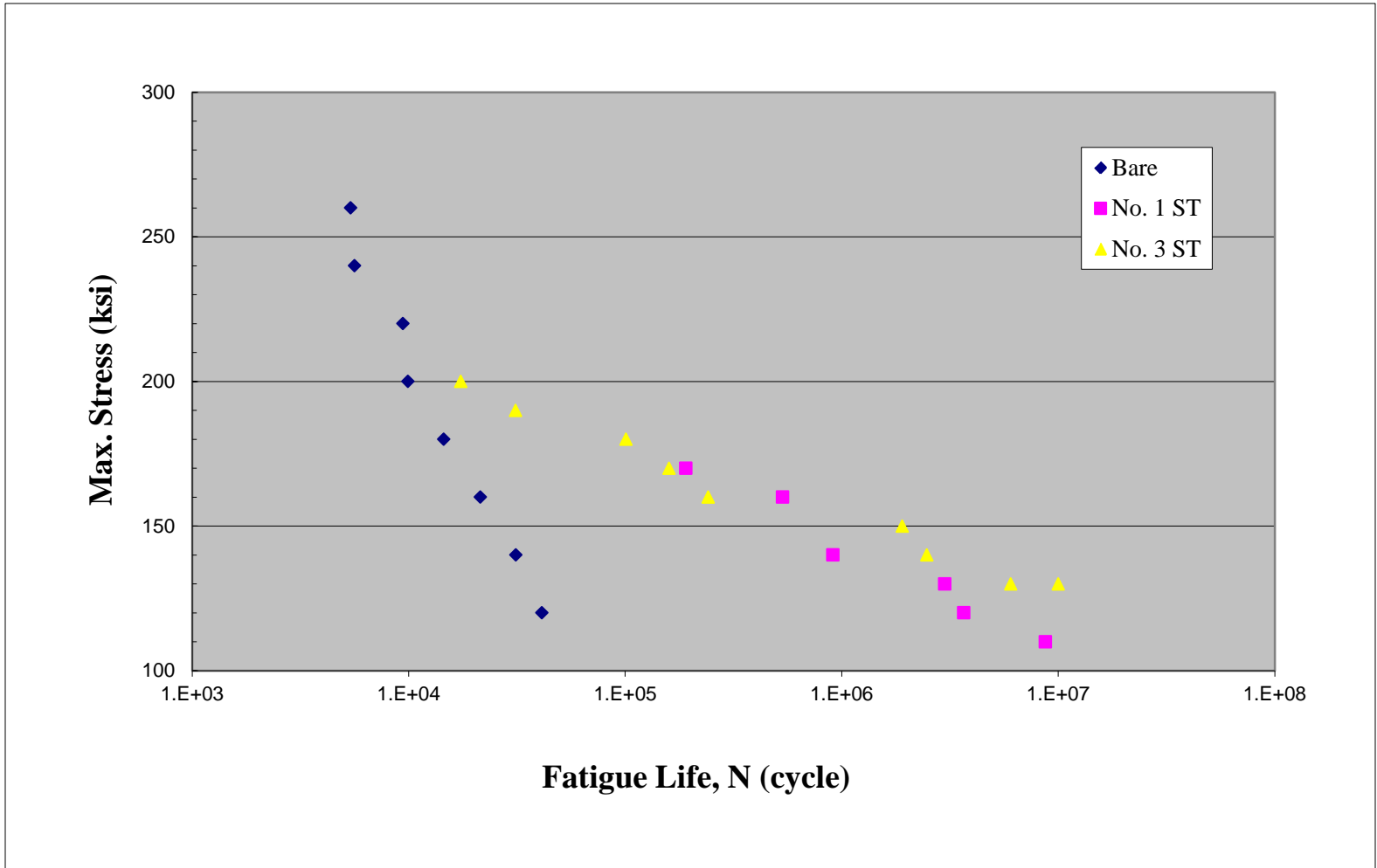
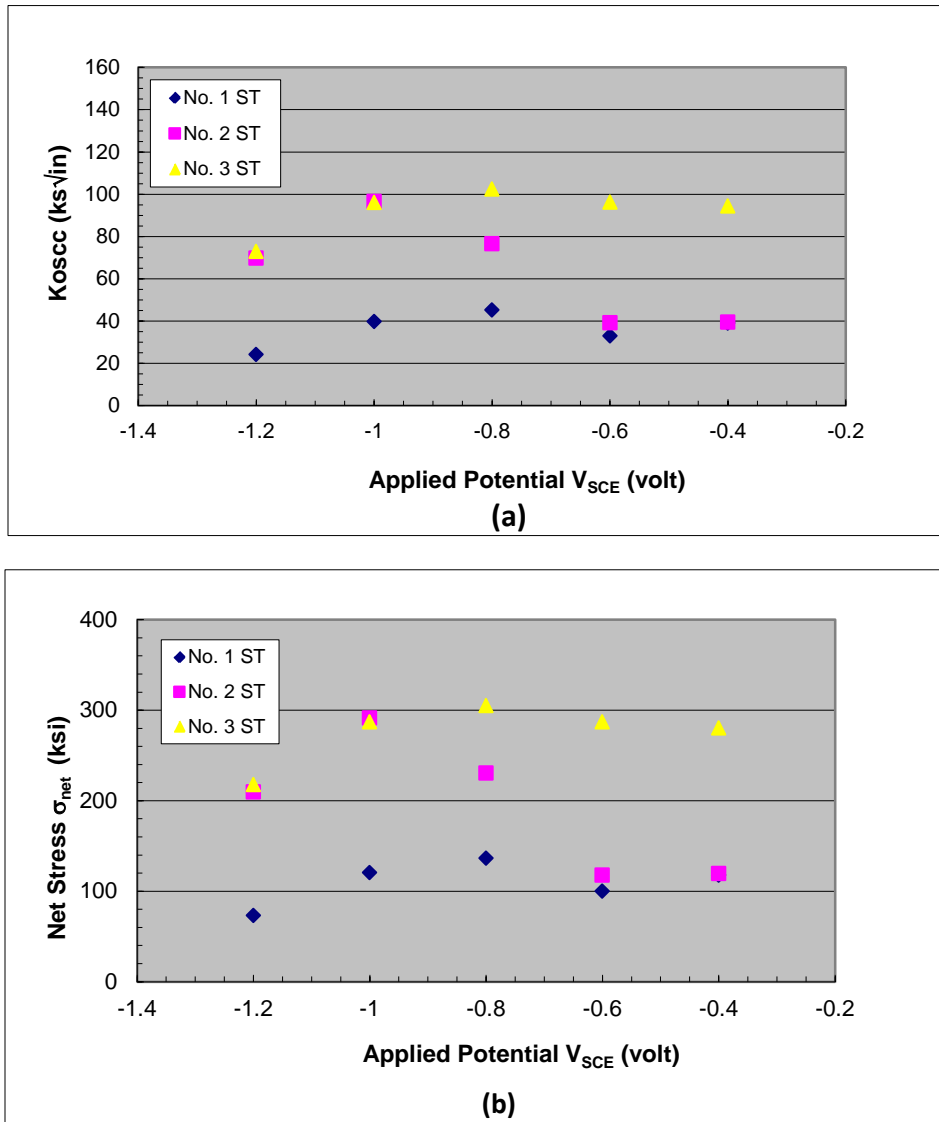Figure 10: Stress-Life Fatigue Curves for Bare and Surface-Treated 4340 Steel Tested in 3.5% NaCl Solution

Figure 11: Variation of Threshold Stress Intensity for SCC K_{OSCC} and Net Stress σ_{net} with Applied Potential V_{SCE}
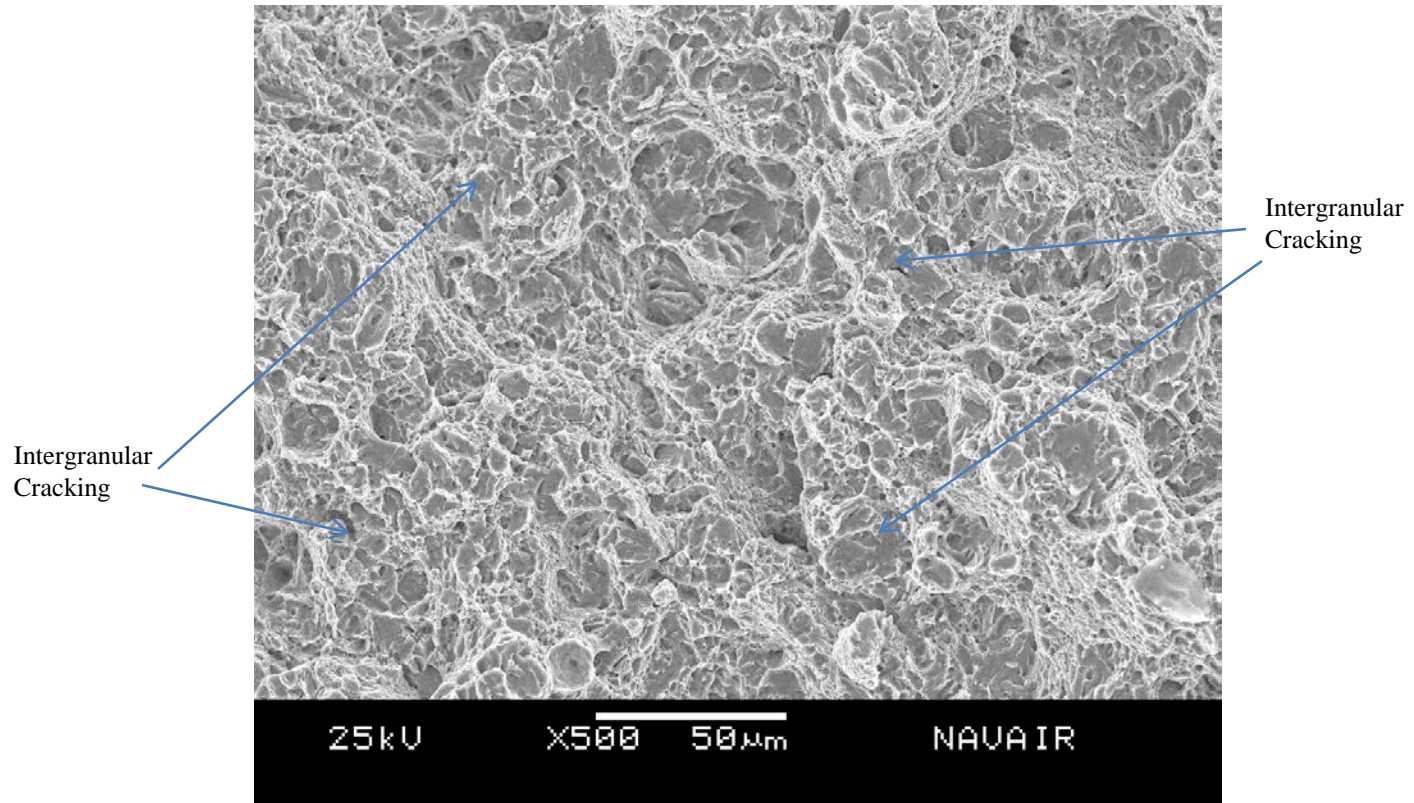(* ST: Surface Treatment)

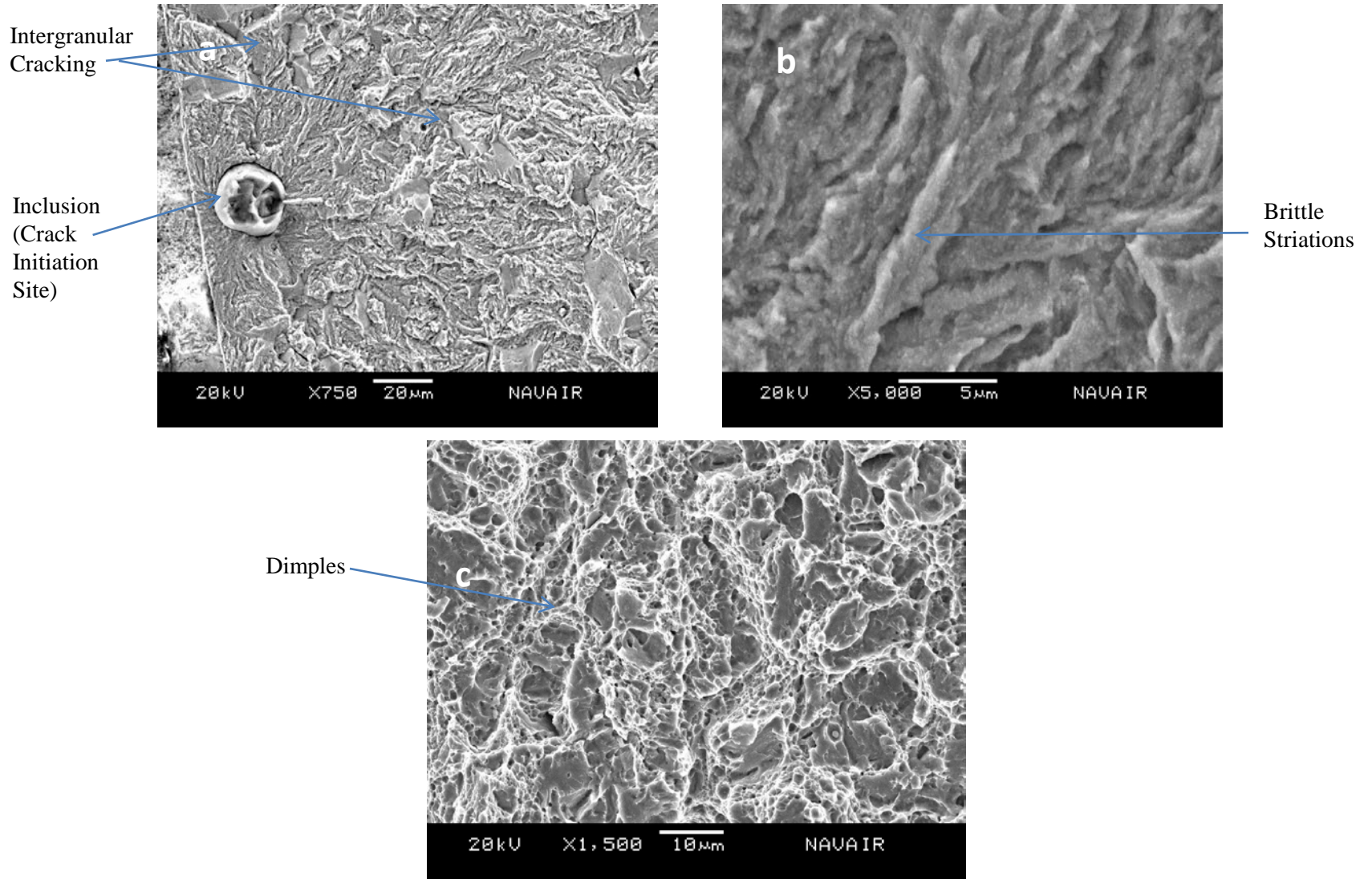Figure 12: SEM Fractograph of No. 2 Surface-Treated Specimen, Fractured under Four-Point Bending in Air

Figure 13: SEM Fractographs of No. 3 Surface-Treated Specimen, Fatigue-Tested in Air
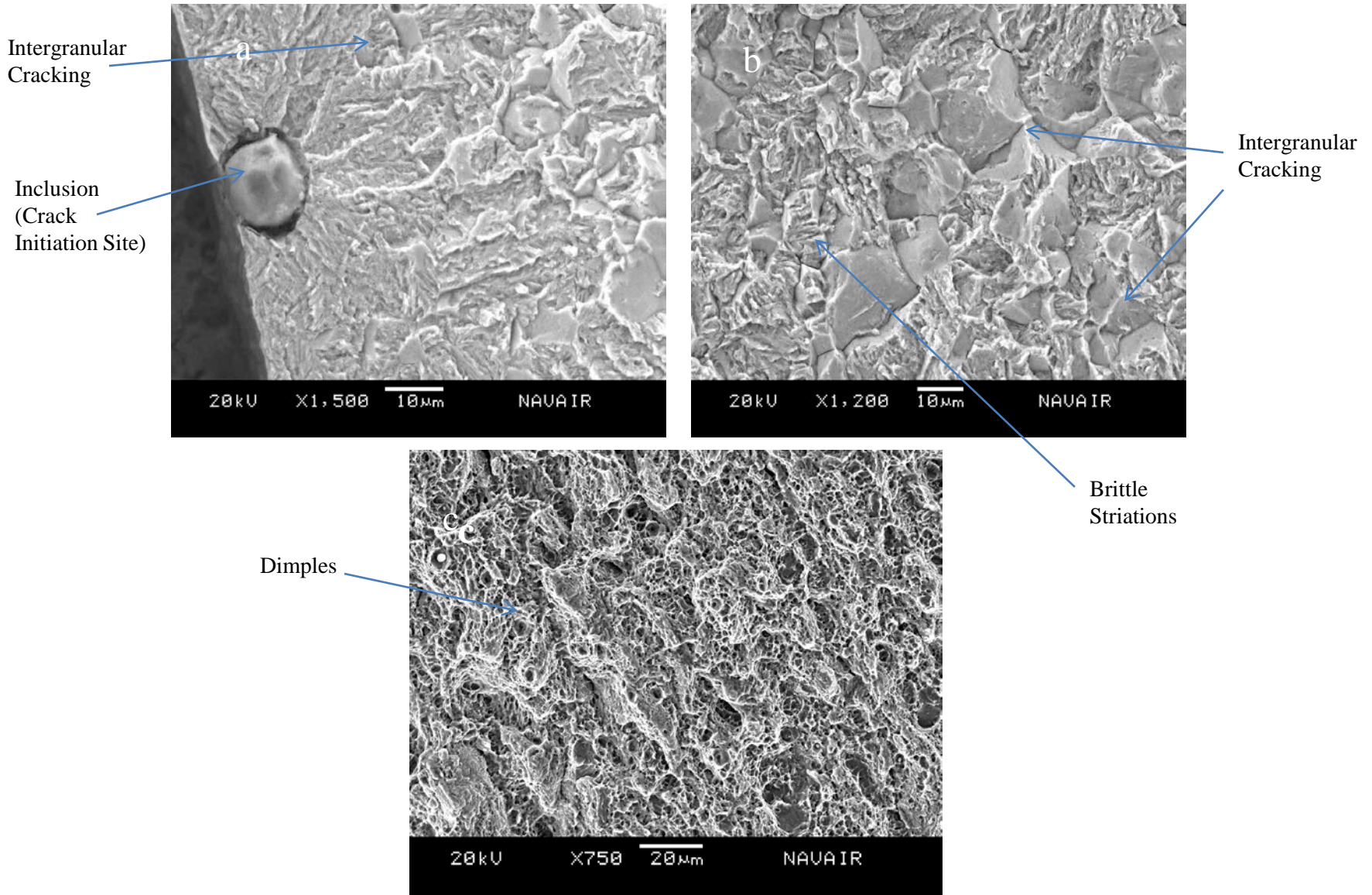
APPENDIX

Figure 14: SEM Fractographs of No. 3 Surface-Treated Specimen, Fatigue-Tested in 3.5% NaCl Solution
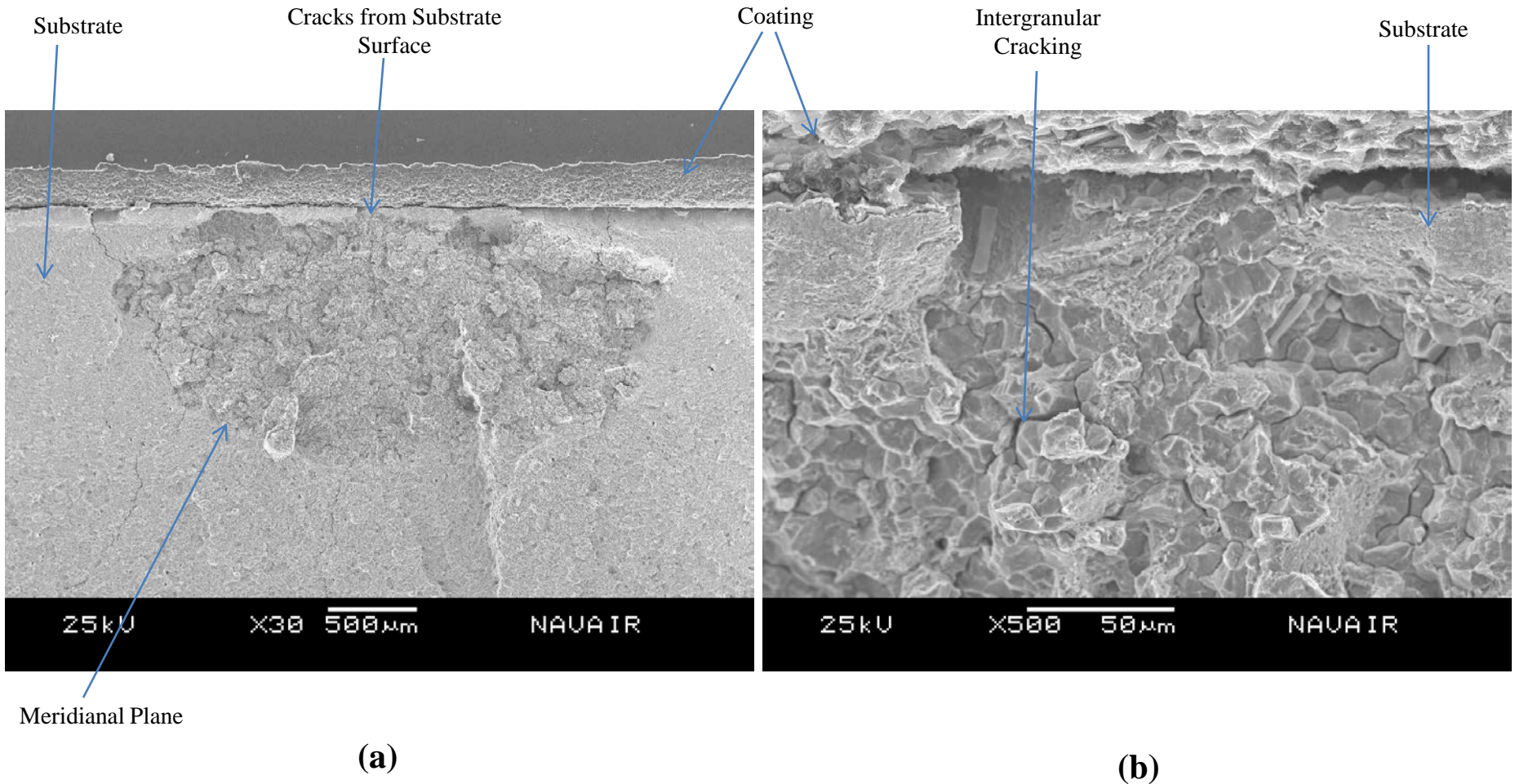
APPENDIX

Figure 15: SEM Fractographs of No. 3 Surface-Treated Specimen, RSL-SCC Tested at V_{SCE} = -1.2 V in 3.5% NaCl Solution

DISTRIBUTION:

NAVAIRSYSCOM (AIR-4.3), Bldg. 2187, Suite 3340   (1)
    48110 Shaw Road, Patuxent River, MD 20670-1906
NAVAIRSYSCOM (AIR-4.3T – Jerry Rubinsky), Bldg. 2187, Suite 3322   (1)
    48110 Shaw Road, Patuxent River, MD 20670-1906
NAVAIRSYSCOM (AIR-4.3.4 – Kevin Kovaleski), Bldg. 2188   (1)
    48066 Shaw Road, Patuxent River, MD 20670-1908
NAVAIRSYSCOM (AIR-4.3.4.1 – Robert Kowalik), Bldg. 2188   (1)
    48066 Shaw Road, Patuxent River, MD 20670-1908
NAVAIRSYSCOM (AIR-4.3.4.1 – Eun U. Lee), Bldg. 2188   (25)
    48066 Shaw Road, Patuxent River, MD 20670-1908
FRC/ISSC Jacksonville (AIR-4.3.4 – John Yadon)   (1)
    Naval Air Station, Jacksonville, FL 32212
FRC/ISSC Jacksonville (AIR 4.3.4.6 – John Benfer)   (1)
    Naval Air Station, Jacksonville, FL 32212
FRC/ISSC Jacksonville (AIR 4.3.4.2 – Luzmarie Youngers)   (1)
    Naval Air Station, Jacksonville, FL 32212
Office of Naval Research (Code 35 - William Nickerson)   (1)
    875 N. Randolph St., Room 1143B, Arlington, VA 22203
NAVAIRWARCENACDIV (4.12.6.2), Bldg. 407, Room 116   (1)\
    22269 Cedar Point Road, Patuxent River, MD 20670-1120
DTIC   (1)
    8725 John J. Kingman Road, Suite 0944, Ft. Belvoir, VA 22060-6218